Grand canonical investigations of prototypical polyelectrolyte models beyond the mean field level of approximation

Stephan A. Baeurle,[1,2,*] Magali Charlot,[3] and Evgenij A. Nogovitsin[4]
[1]*Department of Civil, Environmental and Geomatic Engineering, Institute for Building Materials, ETH, CH-8093 Zurich, Switzerland*
[2]*Department of Chemistry and Pharmacy, Institute of Physical and Theoretical Chemistry, University of Regensburg, D-93053 Regensburg, Germany*
[3]*Advanced Materials Laboratory, Rhodia Recherches et Technologies, 85 rue des Frères Perret, BP 62 - 69192 Saint-Fons Cedex, France*
[4]*Institute of Solution Chemistry, Russian Academy of Sciences, 153045 Ivanovo, Russia*
(Received 21 August 2006; published 31 January 2007)

Understanding the chemistry and physics of polyelectrolyte systems challenges scientists from a wide spectrum of research areas, ranging from colloidal science to biology. However, despite significant progress in the past decades, the calculation of large open polyelectrolyte systems on a detailed level remains computationally expensive, due to the highly polymeric nature of the macromolecules and/or long-range character of the intermonomer interactions. To cope with these difficulties, field-theoretic methodologies based on the mean-field approximation have emerged recently and have proven to provide useful results in the regime of high polyelectrolyte concentration. In this paper we present applications of a low-cost field-theoretic calculation approach based on the method of Gaussian equivalent representation, which has recently been proven useful for delivering accurate results in case of polymer solutions beyond the mean field level of approximation. Here we demonstrate its effectiveness on the example of a Gaussian effective potential, mimicking the effective interactions between weakly charged polyelectrolyte coils, and a screened Coulomb model, describing the effective intermonomer interactions of Debye-Hückel chains. Moreover, we show that the approach opens perspectives to extend the range of applicability of the grand canonical ensemble to dense liquid and solid phases of more sophisticated polyelectrolyte models. Finally, we demonstrate that our approach is also much more reliable for determining the phase boundaries of these models than conventional mean field and grand canonical Monte Carlo approaches.

DOI: 10.1103/PhysRevE.75.011804 PACS number(s): 82.35.Rs, 05.10.−a, 05.20.−y, 05.70.Fh

I. INTRODUCTION

Polyelectrolyte (PE) materials are macromolecular systems that are well known to play a vital role in nature and technology [1]. They are typically composed of long polymeric chains, possessing a multitude of ionizable groups along their backbone that are capable of dissociating in a polar solvent by producing charged species [2]. Among the most prominent examples are the nucleic acids DNA and RNA, which are highly charged biopolyelectrolytes controlling the development and functioning of living cells. However, despite of their importance, systems of PE's remain among the least understood polymeric systems [3]. This relates to the fact that their chemistry and physics is influenced by many controlling parameters, such as molecular weight, salt concentration, *p*H of the solution, etc. Another important characteristic of PE systems is the coexistence of long-range Coulomb and short-range excluded volume interactions. The presence of long-range interactions generally renders their simulation particularly difficult, because of the need for computationally expensive techniques, like the Ewald summation [4]. Moreover, the often highly polymeric nature of PE systems introduces additional complexity by severely slowing down their equilibration [5]. Finally, additional difficulties can occur in the computation of open systems of PE's at lower temperatures in the range of physical interest, because grand canonical algorithms are known to become increasingly inefficient with growing interaction strength between the interacting monomers [6,7]. Since most PE systems, like, e.g., living cells, are open systems where matter and heat exchange between the system and its surroundings does occur, this represents a major drawback on the route towards understanding and predicting their physical properties and behavior.

Most currently available theoretical approaches for treating PE materials are based on particle-based computer simulation methods, like, e.g., molecular dynamics (MD) [8] or Monte Carlo (MC) methods [9]. However, their inherent spatial and temporal limitations prohibit their application to large PE systems characterized by slow equilibration times [5,10], like, e.g., biopolyelectrolytes [11] or block-polyelectrolyte solutions [12]. To cope with these problems, promising alternative techniques to particle-based methods have emerged recently based on a field-theoretic formalism [5,7,13,14]. Field theories for polymers generally make use of the mean-field (MF) approximation [14], which consists in replacing the many-body interaction term in the action by a term where all bodies of the system interact with an average effective field. This reduces any multibody problem into an effective one-body problem and implies that the partition function integral of the model is dominated by a single field configuration. A major benefit of solving problems within the MF approximation is that the estimates provides some useful

*Electronic address: stephan.baeurle@chemie.uni-regensburg.de

insights into the properties and behavior of the system at relatively low computational cost. Originally introduced by Edwards [15] and by Helfand and Tagami [16], MF theories for polymers, also commonly referred to as self-consistent-field theories (SCFT), have been proven useful for estimating structures and thermodynamic properties of a wide variety of polymer systems, including polymer alloys, strongly segregated block copolymers of high molecular weight, molten polymer brushes, etc. [5]. Their applications to PE systems have, however, only been rare [3,17–19]. This is due to the fact that the SCFT formalism is only accurate for highly concentrated PE solutions, where local field fluctuations are averaged out, due to the effective screening of the electrostatic interactions surrounding the monomers [5]. The SCFT provides inaccurate or even qualitatively incorrect results for PE solutions in the regime of low to moderate PE concentrations [5]. Unfortunately, these concentration regimes are highly relevant to biological and industrial applications. In such cases more sophisticated techniques beyond the MF level of approximation are required. One possible solution to the problem is to calculate higher-order corrections to the 0th-order MF approximation. Tsonchev *et al.* developed a MF strategy including leading (one-loop) order fluctuation corrections, to gain new insights into the physics of confined PE solutions [20]. However, in situations where the MF approximation is bad many computationally demanding higher-order corrections to the integral are necessary to get the desired accuracy. Another possibility is to use Monte Carlo (MC) algorithms and to sample the full partition function integral in field-theoretic formulation. However, in a recent work one of the authors (Baeurle) demonstrated that MC sampling in conjunction with the original field-theoretic representation is impracticable due to the so-called *numerical sign problem* [21]. The difficulty is related to the complex and oscillatory nature of the Boltzmann factor, which causes a bad statistical convergence of the functional integral averages of the desired thermodynamic and structural quantities. In such cases special analytical and numerical techniques are necessary to accelerate their statistical convergence [7,21–23]. To make the methodology amenable for computation, Baeurle proposed the contour-shifting technique relying on Cauchy's integral theorem, which was previously successfully employed by Baer *et al.* in field-theoretic electronic structure calculations [24]. Baeurle further demonstrated that, employing this technique in conjunction with the method of Gaussian equivalent representation (GER) of Efimov and Ganbold [25], provides a significant acceleration of the statistical convergence of the functional integral averages in the MC sampling procedure [21]. Other promising beyond MF techniques have been developed recently, but they either still lack the proof of correct statistical convergence [26] or still need to prove their effectiveness in cases where multiple MF solutions are important [27].

The goal of our current paper is to present a new low-cost approximation method based on the method of GER of Efimov and Ganbold [25], which has recently been proven useful in case of polymer solution models [28], and investigate its usefulness for calculating prototypical open PE systems beyond the MF level of approximation. Since the origin of the fluctuation problem in field theories is known to be related to the strength of the effective interactions between the interacting entities [5,7], we test the effectiveness of our method on the example of a Gaussian effective potential, mimicking the effective interactions between weakly charged polyelectrolyte coils, and on a screened Coulomb model, describing the intermonomer interactions of Debye-Hückel chains. We investigate its ability with regard to the MF approach as well as grand canonical Monte Carlo (GCMC) method of Norman *et al.* [29] in providing accurate thermodynamic information.

Our paper is organized in the following way. In Sec. II A we review the basic derivation of the GER of the grand canonical partition function integral and provide its 0th-order approximation as well as the related grand canonical free energy. In Sec. II B we review the MF approximation procedure and derive the corresponding MF representation (MFR) of the partition function integral. Then, in Sec. IV we show applications of these methods to the models, previously introduced in Sec. III, and demonstrate that the 0th-order GER approximation procedure is an effective low-cost approximation strategy for computations within the grand canonical ensemble. Finally, we end our paper with conclusions and a brief outlook.

II. METHODS

A. Gaussian equivalent representation and its 0th-order approximation

The key idea of the GER approach comes from quantum theory and is based on the observation that the main contributions to the partition function integral are provided by low-order tadpole-type Feynman diagrams, which account for contributions due to particle self-interaction. They can effectively be taken into account by rewriting the interaction functional in normal ordered form with respect to a new Gaussian measure and by requiring that the resulting action does not contain any linear and quadratic terms in the field variables. The GER approach was originally devised by Efimov and Ganbold for the analytical calculation of functional integrals over the Gaussian measure [25] and has successfully been applied in several areas of quantum physics [30]. In a subsequent work Efimov and Nogovitsin utilized this strategy for the calculation of partition function integrals and distribution functions of various classical many-particle systems, belonging to the canonical and grand canonical ensemble [31]. Here, we use the method to reformulate the original field-theoretic representation of the grand canonical partition function integral in its corresponding GER and to extract its 0th-order approximation. To begin, let us consider the grand canonical partition function in particle representation,

$$\Xi(z,V,\beta)=\sum_{N=0}^{\infty}\frac{z^N}{N!}\int_V d\mathbf{r}_1\cdots\int_V d\mathbf{r}_N\exp\left(-\beta\sum_{i<j}\Phi(\mathbf{r}_i-\mathbf{r}_j)\right), \tag{1}$$

for a system of volume V, kept fixed at an inverse temperature β and activity $z=[2\pi m/(\beta h^2)]^{3/2}e^{\beta\mu}$, in which the pair potential $\Phi(\mathbf{r}_i-\mathbf{r}_j)$ describes the two-body interactions be-

tween the particles. This expression can easily be rewritten in the basic field-theoretic representation [31,32]

$$\Xi(z,V,\beta) = \int d\mu_\Phi[\phi]\exp\left(z\int_V d\mathbf{r}{:}e^{i\sqrt{\beta}\phi(\mathbf{r})}{:}_\Phi\right) = \int \frac{\delta\phi}{\sqrt{\det\Phi}} e^{-S[\phi]}, \tag{2}$$

where the action

$$S[\phi] = \frac{1}{2}(\phi\Phi^{-1}\phi) - z\int_V d\mathbf{r}{:}e^{i\sqrt{\beta}\phi(\mathbf{r})}{:}_\Phi, \tag{3}$$

while the Gaussian measure is defined in a standard way as [31]

$$d\mu_\Phi[\phi] = \frac{\delta\phi}{\sqrt{\det\Phi}}\exp\left(-\frac{1}{2}(\phi\Phi^{-1}\phi)\right),$$

$$\int d\mu_\Phi[\phi] = 1,$$

$$\frac{1}{\sqrt{\det\Phi}} \overset{V\to R^3}{=} \exp\left(-\frac{V}{2}\int\frac{d\mathbf{p}}{(2\pi)^3}\ln\Phi(\mathbf{p})\right),$$

$$\frac{1}{V^2}\int d\mathbf{r}'\Phi(\mathbf{r},\mathbf{r}')\Phi^{-1}(\mathbf{r}',\mathbf{r}'') = \delta(\mathbf{r}-\mathbf{r}''), \tag{4}$$

with the short-hand notation $(\phi\Phi^{-1}\phi) = 1/V^2\int_V d\mathbf{r}\int_V d\mathbf{r}'\,\phi(\mathbf{r})\Phi^{-1}(\mathbf{r}-\mathbf{r}')\phi(\mathbf{r}')$. The Fourier transform of the pair potential is given by $\tilde{\Phi}(\mathbf{p}) = \int d\mathbf{r}\Phi(\mathbf{r})\exp(-i\mathbf{pr}) = \Phi(\mathbf{p})V$ with $\Phi(\mathbf{r}) = \int d\mathbf{p}/(2\pi)^3\tilde{\Phi}(\mathbf{p})\exp(i\mathbf{pr})$. For simplicity, we have assumed in the previous formulas that the Fourier transform of the potential is positive, i.e., $\tilde{\Phi}(\mathbf{p}) > 0$. It is, however, worth mentioning that the formalism can easily be extended to potentials with additional negative Fourier coefficients $\tilde{\Phi}(\mathbf{p}) < 0$ by introducing a supplementary field variable [22]. Moreover, in Eq. (2) we have introduced the conception of normal product according to the given Gaussian measure $d\mu_\Phi[\phi]$, namely,

$${:}e^{i\sqrt{\beta}\phi(\mathbf{r})}{:}_\Phi = e^{i\sqrt{\beta}\phi(\mathbf{r})}e^{(\beta/2)\Phi(0)},$$

$$\phi(\mathbf{r})\phi(\mathbf{r}') = {:}\phi(\mathbf{r})\phi(\mathbf{r}'){:}_\Phi + \Phi(\mathbf{r}-\mathbf{r}'), \tag{5}$$

which means in other words,

$$\int d\mu_\Phi[\phi]{:}e^{i\sqrt{\beta}\phi(\mathbf{r})}{:}_\Phi = 1. \tag{6}$$

The key idea of the GER approach is that the main contribution to the functional integral in Eq. (2), provided by low-order tadpole-type Feynman diagrams, should be concentrated in a new quadratic Gaussian measure $d\mu_D[\phi]$. This is achieved by displacing the field variable using Cauchy's integral theorem,

$$\phi(\mathbf{r}) \to \phi(\mathbf{r}) + i\frac{c^{\mathrm{GER}}(\mathbf{r})}{\sqrt{\beta}}, \tag{7}$$

where $c^{\mathrm{GER}}(\mathbf{r})$ represents the shifting function, and by rewriting the resulting contour-shifted representation with respect to the new potential $D(\mathbf{r},\mathbf{r}')$. As a consequence, the functional integral in Eq. (2) adopts the following form:

$$\Xi(z,V,\beta) = \int d\mu_D[\phi]e^{-S'[\phi]}, \tag{8}$$

with

$$S'[\phi] = -\ln\sqrt{\frac{\det D}{\det\Phi}} - \frac{1}{2\beta}(c^{\mathrm{GER}}\Phi^{-1}c^{\mathrm{GER}}) + \frac{1}{2}(\phi[\Phi^{-1}-D^{-1}]\phi) + \frac{i}{\sqrt{\beta}}(\phi\Phi^{-1}c^{\mathrm{GER}}) - zA\int_V d\mathbf{r}e^{-c^{\mathrm{GER}}(\mathbf{r})}e^{i\sqrt{\beta}\phi(\mathbf{r})}e^{(\beta/2)D(0)}, \tag{9}$$

where $A = \exp\left(\frac{\beta}{2}[\Phi(0)-D(0)]\right)$. Here, the new Gaussian measure is defined as

$$d\mu_D[\phi] = \frac{\delta\phi}{\sqrt{\det D}}\exp\left(-\frac{1}{2}(\phi D^{-1}\phi)\right),$$

$$\int d\mu_D[\phi] = 1,$$

$$\frac{1}{V^2}\int_V d\mathbf{r}'D^{-1}(\mathbf{r},\mathbf{r}')D(\mathbf{r}'-\mathbf{r}'') = \delta(\mathbf{r}-\mathbf{r}''),$$

$$D(\mathbf{r}-\mathbf{r}') = \int d\mu_D[\phi]\phi(\mathbf{r})\phi(\mathbf{r}'),$$

$$\frac{1}{\sqrt{\det D}} \overset{V\to\mathrm{R}^3}{=} \exp\left(-\frac{V}{2}\int\frac{d\mathbf{p}}{(2\pi)^3}\ln D(\mathbf{p})\right). \tag{10}$$

Now, to concentrate the main contribution to the functional integral in Eq. (8) in the new quadratic Gaussian measure $d\mu_D[\phi]$, we take into account that the linear and quadratic terms in the field variable $\phi(\mathbf{r})$ should vanish in the action $S'[\phi]$, given in Eq. (9). As a result, we obtain two equations, defining the GER potential $D(\mathbf{r}-\mathbf{r}')$ and contour-shifted parameter $c^{\mathrm{GER}}(\mathbf{r})$ [31,33],

$$zA\int_V d\mathbf{r}e^{-c^{\mathrm{GER}}(\mathbf{r})}\phi(\mathbf{r}) - \frac{1}{\beta}(\phi\Phi^{-1}c) = 0,$$

$${:}\left\{\beta zA\int_V d\mathbf{r}e^{-c^{\mathrm{GER}}(\mathbf{r})}\phi^2(\mathbf{r}) + (\phi[\Phi^{-1}-D^{-1}]\phi)\right\}{:}_D = 0. \tag{11}$$

These equations can be reformulated as

$$c^{\mathrm{GER}}(\mathbf{r}) = \beta z A \int_V d\mathbf{r}' \Phi(\mathbf{r}-\mathbf{r}') e^{-c^{\mathrm{GER}}(\mathbf{r}')},$$

$$D(\mathbf{r},\mathbf{r}'') = \Phi(\mathbf{r}-\mathbf{r}'') - \beta z A \int_V d\mathbf{r}' \Phi(\mathbf{r}-\mathbf{r}') e^{-c^{\mathrm{GER}}(\mathbf{r}')} D(\mathbf{r}',\mathbf{r}''), \tag{12}$$

and solved self-consistently for the shifted-contour parameter $c^{\mathrm{GER}}(\mathbf{r})$ and the potential $D(\mathbf{r},\mathbf{r}')$. For homogeneous solutions and in the limit $V \to R^3$ both functions become translation invariant, i.e.,

$$c(\mathbf{r}) = c = \mathrm{const}, \quad D(\mathbf{r},\mathbf{r}') = D(\mathbf{r}-\mathbf{r}'). \tag{13}$$

Consequently, the first expression in Eq. (12) takes the form

$$c^{\mathrm{GER}} - \frac{\beta}{2}[\Phi(0) - D(0)] - \ln\left(\frac{\beta\tilde{\Phi}(\mathbf{p}=0)z}{c^{\mathrm{GER}}}\right) = 0, \tag{14}$$

while the second expression gives

$$\tilde{D}(\mathbf{p}) = \tilde{\Phi}(\mathbf{p}=0)\frac{v(\mathbf{p})}{1+cv(\mathbf{p})}, \tag{15}$$

with $v(\mathbf{p}) = \tilde{\Phi}(\mathbf{p})/\tilde{\Phi}(\mathbf{p}=0)$. These formulas determine the shifted-contour parameter $c = c(z,\beta)$ as a function of z, β, as well as the GER potential $D(\mathbf{r}-\mathbf{r}')$. As a result, we obtain the GER of the grand canonical partition function

$$\Xi(z,V,\beta) = e^{-\beta\Omega^0_{\mathrm{GER}}} \int d\mu_D[\phi] e^{W[\phi]}, \tag{16}$$

where

$$W[\phi] = \frac{c^{\mathrm{GER}}}{\beta\tilde{\Phi}(\mathbf{p}=0)} \int_V d\mathbf{r} e_2^{i\sqrt{\beta}\phi(\mathbf{r})} \tag{17}$$

and

$$e_2^{i\sqrt{\beta}\phi(\mathbf{r})} = e^{i\sqrt{\beta}\phi(\mathbf{r})+(\beta/2)D(0)} - 1 - i\sqrt{\beta}\phi(\mathbf{r}) + \frac{\beta}{2}[\phi^2(\mathbf{r}) - D(0)]. \tag{18}$$

The function Ω^0_{GER} defines the grand canonical free energy in the 0th-order GER (GER0) approximation and is given by

$$\Omega^0_{\mathrm{GER}} = -\frac{V}{2\beta}\int \frac{d\mathbf{p}}{(2\pi)^3}\left(\ln\frac{\tilde{D}(\mathbf{p})}{\tilde{\Phi}(\mathbf{p})} - \frac{\tilde{D}(\mathbf{p})}{\tilde{\Phi}(\mathbf{p})} + 1\right) - \frac{V(2c^{\mathrm{GER}} + c^{\mathrm{GER2}})}{2\beta^2\tilde{\Phi}(\mathbf{p}=0)}. \tag{19}$$

The corresponding thermodynamic and structural quantities can now easily be derived by using the standard thermodynamic relations in conjunction with the GER0 approximation of the partition function integral,

$$\Xi^0_{\mathrm{GER}} = \exp(-\beta\Omega^0_{\mathrm{GER}}), \tag{20}$$

which will in the following be referred to as the free-energy route (F route), or using the standard thermodynamic expressions defined via the radial distribution function, which will be called the $g(r)$ route. For more details we refer to Appendix A. We point out that the function Ω^0_{GER} explicitly depends on the parameters β and c^{GER}, while only implicitly on the activity z. The activity enters through the shifting function $c^{\mathrm{GER}} = c^{\mathrm{GER}}(z,\beta)$ defined via Eq. (14). Moreover, we point out that in the GER the effective coupling constant is connected with β and the characteristics of the potential $\Phi(\mathbf{r})$, as we can easily deduce from Eq. (17). Finally, it is worth mentioning that the GER of the partition function in Eq. (16) is physically fully equivalent to the field-theoretic representation given in Eq. (2), while possessing better approximation characteristics.

B. Mean-field representation and its 0th-order approximation

The goal of the MF contour-shifting procedure is to distort the original integration path of the partition function integral in such way that one captures MF configurations, which provide relevant contributions to the overall integral entity for the external conditions under consideration. For example, the homogeneous MF solution characterizes the liquid phase of the model system under consideration, while other MF solutions characterize other thermodynamic phases [22]. Similarly as in case of the method of GER in Sec. II A, a representation of the partition function shifted through the relevant MF configuration can be derived and one obtains the corresponding mean-field representation MFR. In essence, the technique consists in reformulating the partition function integral in Eq. (2) by performing a suitable contour shift into the complex plane using Cauchy's integral theorem,

$$\phi(\mathbf{r}) \to \phi(\mathbf{r}) + i\frac{c^{\mathrm{MF}}(\mathbf{r})}{\sqrt{\beta}}, \tag{21}$$

where $c^{\mathrm{MF}}(\mathbf{r})$ represents the shifting function. As a result, one obtains the contour-shifted formulation of the grand canonical partition function $\Xi(z,V,\beta) = \int d\mu_\Phi[\phi] \exp[-S(\phi + ic^{\mathrm{MF}}/\sqrt{\beta})] = \int d\mu_\Phi[\phi] \exp[-S[\phi]]$, which is again physically fully equivalent to the basic field-theoretic representation defined in Eq. (2). For example, the shift through the homogeneous MF configuration is obtained by applying the stationary condition

$$\left.\frac{\delta S[\phi]}{\delta\phi}\right|_{\phi(\mathbf{r})=\phi^{\mathrm{MF}}(\mathbf{r})} = 0, \tag{22}$$

where $\phi^{\mathrm{MF}}(\mathbf{r}) = ic^{\mathrm{MF}}(\mathbf{r})/\sqrt{\beta}$ represents the MF solution, and assuming a homogeneous solution,

$$\phi^{\mathrm{MF}}(\mathbf{r}) = \phi^{\mathrm{MF}}(\mathbf{p}=0) = i\frac{c^{\mathrm{MF}}(\mathbf{p}=0)}{\sqrt{\beta}}. \tag{23}$$

As a result, we get the following equation:

$$c^{\mathrm{MF}} = \beta z e^{(\beta/2)\Phi(0)}\tilde{\Phi}(\mathbf{p}=0)e^{-c^{\mathrm{MF}}}. \tag{24}$$

The 0th-order approximation of the MFR is the standard MF approximation of the grand canonical partition function, which takes the form

$$\Xi^0_{\mathrm{MF}}(z,V,\beta) = e^{-S[c^{\mathrm{MF}}]}. \tag{25}$$

Analogously as in the case of the GER0 approach, the corresponding structural and thermodynamic quantities can now easily be derived by using the standard thermodynamic expressions in conjunction with the MF approximation of the partition function integral given in Eq. (25) or the free energy defined via $\Xi^0_{\mathrm{MF}}=\exp(-\beta\Omega^0_{\mathrm{MF}})$, where Ω^0_{MF} denotes the 0th-order MF approximation of the grand canonical free energy (F route). Alternatively, one can also use the standard thermodynamic relations defined via the radial distribution function [$g(r)$ route]. For more details, we refer to Appendix B. In recent investigations [21,23] Baeurle showed that, approaching the phase transitions of the system, other configurations than the MF configuration of the respective phase may become important and that, as a consequence, a MF shift is not necessarily the most optimal shift with respect to statistical convergence in the MC sampling procedure. Moreover, he demonstrated that the method of GER does take this fact into account and provides an improved shift, leading to a significant acceleration of the statistical convergence in the low temperature and/or large system size regime [21].

III. MODELS

A useful theoretical approach that greatly facilitates the computation of polymers and complex fluids is the concept of effective interactions between suitably chosen degrees of freedom in the system under study [2,7,34]. In particular, the concept was recently found to be very useful in the calculation of structure and thermodynamics of a wide variety of soft matter systems [35]. For instance, Louis *et al.* [34] have shown that it provides accurate structural and thermodynamic information of polymer solutions under good solvent conditions. To this end, they demonstrated that self-avoiding walk polymer chains immersed in a good solvent form highly penetrable coils and that the effective pair interactions between their center of mass can well be represented by a repulsive Gaussian potential of the form [36]

$$\Phi(r) = \Phi(0)\exp[-(r/R)^2], \tag{26}$$

where $r=|\mathbf{r}|$ is the distance between the interacting coils, while $\Phi(0)$ and R are the energy scale and width of the Gaussian, respectively. In their investigations they demonstrated that this model accurately reproduces the structural and thermodynamic properties of such systems over the entire concentration range. In a recent work, Konieczky *et al.* could further show that it also reproduces the characteristic thermodynamic features of solutions of weakly charged PE chains, forming highly penetrable coils as in case of polymer solutions, and, thus, constitutes a useful potential model to mimic their effective interactions [2]. By direct comparison of computer simulation results and heat capacity measurements, Baeurle and Kroener have lately shown that the Gaussian effective potential also reproduces the characteristic thermodynamic features of micellar aggregates of ionic surfactants [10]. These findings have recently found additional support through several theoretical and experimental investigations on similar systems [37]. In the following we investigate the effectiveness of the GER0 approximation in providing accurate thermodynamic information for PE solutions, described through this example model. Note that in all our calculations, presented in the following, we employed the system of reduced units (r.u.) that is natural for the model [21].

In the subsequent part of this work we apply the GER0 approximation to the screened Coulomb model, describing the effective interactions between Debye-Hückel chains [38]. We performed our investigations on this intermonomer interaction model, because the origin of the fluctuation problem in field theories is well known to be related to the strength of the effective interactions between the interacting monomers [5,7]. Since the pioneering theory of Derjaguin, Landau, Verwey, and Overbeek (DLVO) [7,39], it is well established that the effective interactions between monomers of PE's can well be described by a Debye-Hückel (DH) or Yukawa potential of the following form [38]:

$$\Phi(r) = \Phi_0\left(\frac{a}{r}\right)\exp(-\kappa r), \tag{27}$$

where r is the distance between the monomer centers and a is a typical intermonomer distance. The prefactor Φ_0 is proportional to the effective charges of the interacting monomers, while the DH screening parameter κ governs the range of interactions and is a function of the density of the screening ions as well as the dielectric properties of the solution [38]. In this context, it is also worth mentioning that the DH or Yukawa potential has also been used to model the interactions of a multitude of other physical systems, ranging from elementary particle physics to colloidal suspensions [38,40,41]. Note that, since the potential is singular at the origin, we regularize it by the replacement $\Phi(r)\rightarrow\Phi(r+\epsilon)$ and assume that ϵ is a vanishingly small parameter. Moreover, in all our calculations, presented in the following, we employ the system of reduced units that is natural for the model, i.e., a, $\Phi(\epsilon\rightarrow 0+)/k_B$, $\Phi(\epsilon\rightarrow 0+)$, and $\Phi(\epsilon\rightarrow 0+)/a^3$ are adopted as units of length, temperature, energy, and pressure, respectively.

IV. RESULTS AND DISCUSSION

We start our investigations by computing important thermodynamic quantities for the Gaussian PE model using our low-cost approximation methods introduced previously. We compare the delivered results to nonapproximated ones generated with the grand canonical Monte Carlo GCMC technique of Norman *et al.* [29]. The GCMC technique relies on the conventional Metropolis MC algorithm [4], to perform the particle displacements. To simulate the particle exchange between the physical system and the particle bath, it incorporates a supplementary particle creation and destruction step into the algorithm. In Fig. 1 we show the results obtained for the average PE coil density and corresponding relative error using the GER0, MF as well as GCMC method as a function of the activity-related parameter $B=\ln(zV)$ at a temperature of $T^*=0.05$. We observe that the MF results deviate much more significantly from the GCMC results with

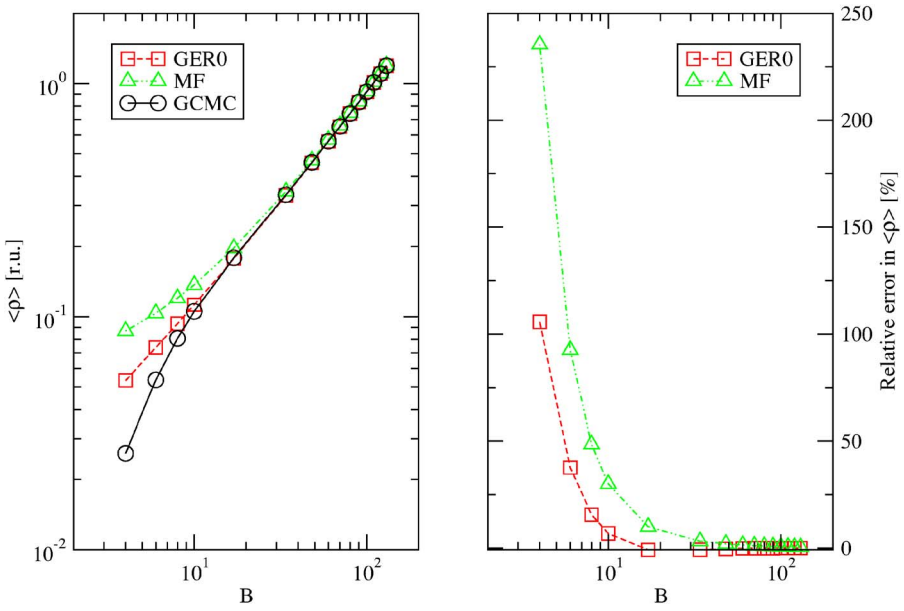

FIG. 1. (Color online) Average PE coil density and corresponding relative error as a function of the μ-related parameter B for the Gaussian PE model. All error bars of the GCMC results are smaller than symbol size.

decreasing B parameter than the GER0 results. At the smallest B parameter under consideration, the relative error in the average density obtained with the MF approximation is more than 2 times as large as the error obtained with the GER0 approximation and the discrepancy increases steadily. Next, in Fig. 2 we plot the negative of the grand canonical free energy and the corresponding relative error as a function of the B parameter for the same model, using a volume of $V^*=864$ and the same temperature as previously. Note that we plotted the negative of the free energy for a better visualization on a logarithmic scale. Again, we observe that the GER0 results are significantly more accurate with decreasing B parameter than the MF results. From the graph visualizing the corresponding relative error, we can deduce that the benefit in accuracy of the GER0 method increases steeply with decreasing B parameter compared to the MF method. At the smallest B parameter under consideration, the relative error of the MF approximation is about 5 times larger than the error obtained with the GER0 approximation. This is due to the fact that the GER0 approximation method introduces a tremendous amount of correlation into the calculation in contrast to the MF approach [28,42], which does not take into account any correlation at all. The slight deviations of the GER0 results from the GCMC results at small B parameter are caused by the neglection of the higher-order corrections to the free energy given by $W[\phi]$ in Eq. (17), which become increasingly important with decreasing B parameter and, thus, need to be taken into account to achieve a higher accuracy in the approximation. These higher-order corrections can, e.g., be computed using the GER formalism in conjunction with the Metropolis MC algorithm, as demonstrated by Baeurle *et al.* in the references [21,32]. Next, we calculate the thermodynamic properties for the DH intermonomer interaction model, selecting the following potential parameters

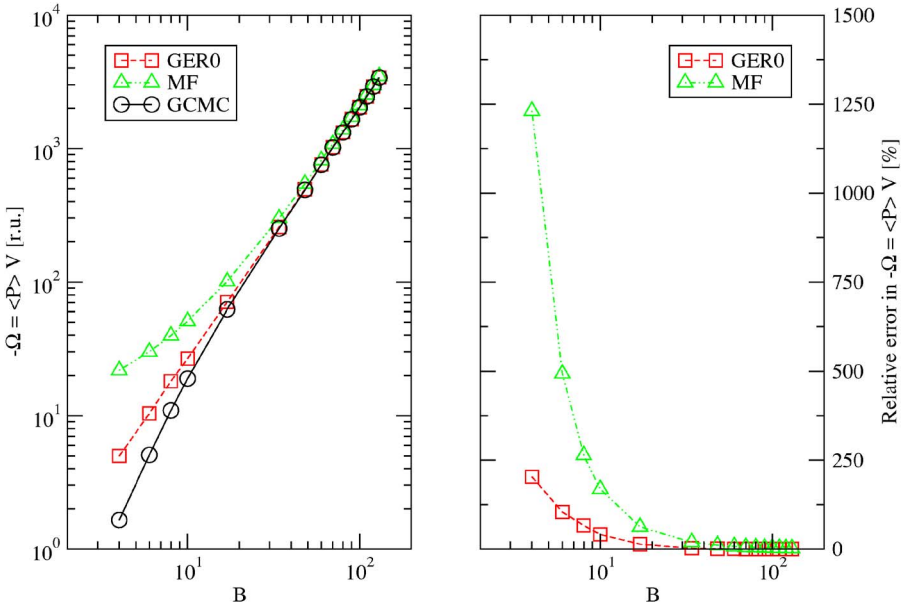

FIG. 2. (Color online) Grand canonical free energy and corresponding relative error as a function of the μ-related parameter B for the Gaussian PE model. All error bars of the GCMC results are smaller than symbol size.

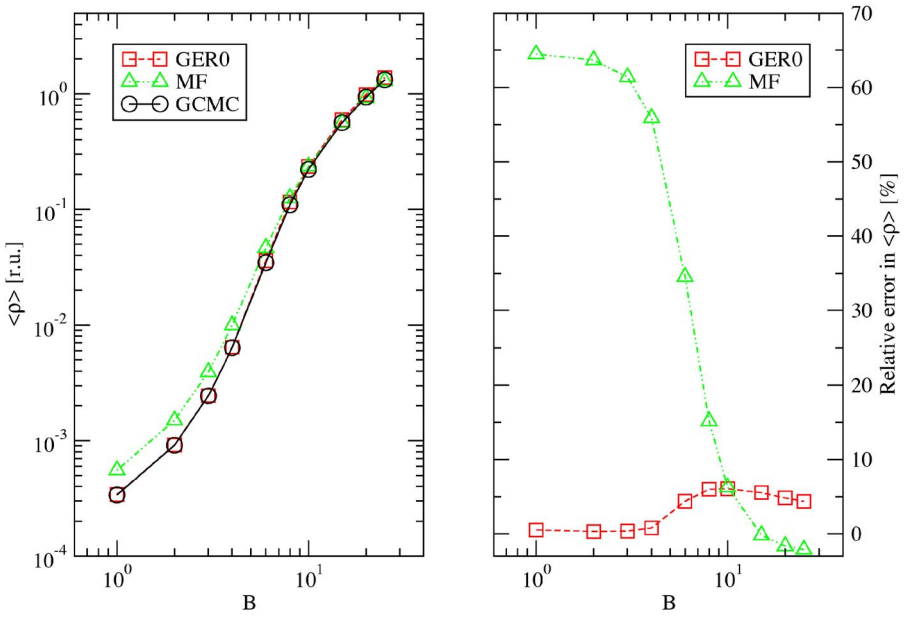

FIG. 3. (Color online) Average monomer density and corresponding relative error as a function of the μ-related parameter B for the DH intermonomer interaction model. All error bars of the GCMC results are smaller than symbol size.

$\Phi_0^*=1$, $\kappa^*=1$ and using the same calculation methods as for the Gaussian PE model. In Fig. 3 we visualize the results obtained for the average monomer density as a function of the B parameter at a temperature of $T^*=1$, using the GER0 and MF approximation methods as well as the GCMC method of Norman *et al.* We observe that the MF results deviate increasingly with decreasing B parameter with respect to the GCMC results, while the GER0 results agree well over the whole parameter range. In contrast to the Gaussian PE model, the relative error in the average density of the MF approximation reaches a plateau in the lower B-parameter range. The maximum discrepancy between the relative errors of the MF and GER0 approximation methods in the small B-parameter range amounts to 65%. Next, in Fig. 4 we plot the corresponding grand canonical free energy using a volume of $V^*=8000$ as a function of the B parameter. Again, we observe that the MF results deviate increasingly with decreasing B parameter with regard to the GCMC results, while the GER0 results coincide well with the GCMC results over the whole parameter range. Similarly as in case of the average density, the maximum discrepancy between the relative errors of the MF and GER0 approximation methods in the small B-parameter range amounts to 65%. Furthermore, it is worth noting that the GER0 curves of the average density and free energy show minor deviations in the intermediate B-parameter range with a maximum deviation at $B=10$. This demonstrates that the accuracy of the GER0 approximation correlates with the strength of the effective interactions, which is the largest in the intermediate B-parameter range [7]. This can easily be explained by the fact that for small B parameters the density of the monomers is low and the interactions between the monomers are only small, while for large B parameters the concentration of the monomers is so large that tremendous screening of the inter-

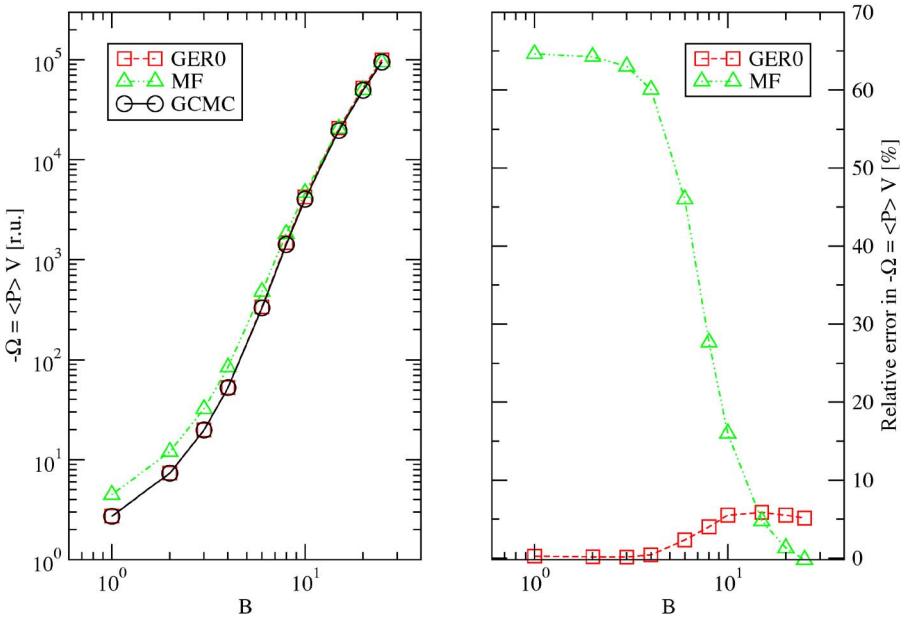

FIG. 4. (Color online) Grand canonical free energy and corresponding relative error as a function of the μ-related parameter B for the DH intermonomer interaction model. All error bars of the GCMC results are smaller than symbol size.

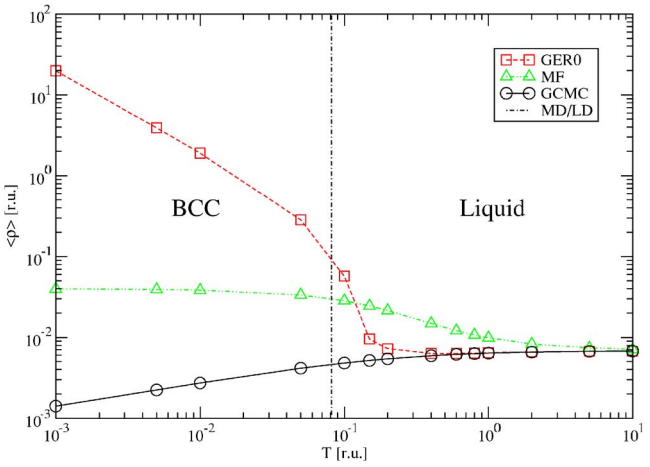

FIG. 5. (Color online) Average monomer density as a function of the temperature for the DH intermonomer interaction model. All error bars of the GCMC results are smaller than symbol size.

actions does occur, which leads to a reduced correlation in the high concentration limit. In this context, it is also worth pointing out that the MF results do not show this behavior, because the MF approximation does not take into account any correlation at all. Next, in Figs. 5 and 6 we visualize the average density and the corresponding grand canonical free energy for the same model at a constant B parameter of $B=4.0$ and a volume of $V^*=8000$ as a function of temperature, computed with the same calculation methods as previously. We calculated the GER0 results for the free energy using the GER0 approximation expressions, derived via the F route or $g(r)$ route in Appendix A. In addition, we show the location of the liquid-solid phase transition, which only depends on the temperature, determined by Robbins *et al.* [41] using microcanonical molecular dynamics (MD) and lattice dynamics (LD) calculations. In this context, it is worth noting that the phase diagram of the repulsive DH potential is characterized by a liquid-solid and solid-solid phase transitions, which take place among the three stable phases of the

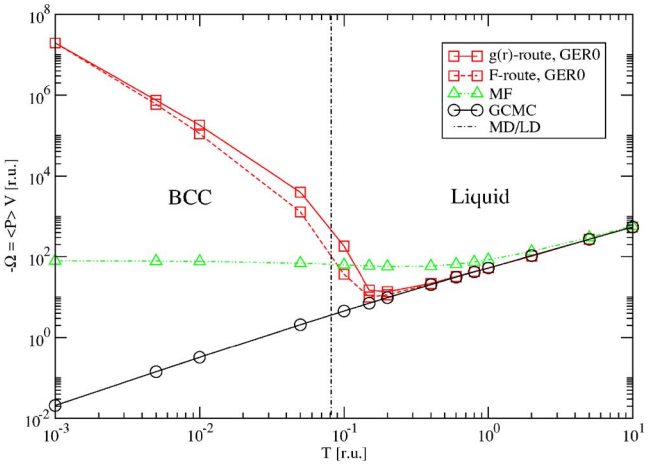

FIG. 6. (Color online) Grand canonical free energy as a function of the temperature for the DH intermonomer interaction model. All error bars of the GCMC results are smaller than symbol size.

potential, i.e., the liquid, body-centered-cubic (BCC) and face-centered-cubic (FCC) phases [41]. Moreover, a vapor-liquid phase transition has recently been discovered by Dijkstra and van Roij for this model in a certain range of potential parameters Φ_0 and κ [43]. However, it has also been demonstrated in their investigation that for the values of potential parameters, considered in our work, only a fluid phase does exist. From both figures, we deduce that the curves of the average density and grand canonical free energy, computed with the GER0 method, coincide well with the GCMC simulation data for temperatures $T^*>0.4$. At smaller temperatures, the GER0 curves deviate increasingly, until they undergo a severe jump of several orders of magnitude at $T^*\approx 0.15$. We note that the temperature of the jump almost coincides with the temperature of the liquid-solid phase transition at $T^*\approx 0.08$, determined through MD and LD calculations. From the graphs, we further infer that at this temperature a discontinuity in the first-order derivatives of the average density and grand canonical free energy with respect to temperature does appear, which is typical for a first-order phase transition. Since, as previously discussed, this model for the potential parameters under consideration does not possess a vapor-liquid transition, we conclude that the GER0 curves at this temperature reproduce the characteristic features of the liquid-BCC phase transition of the model. In contrast to that, the curve of the average density, calculated with the MF approximation, grows only smoothly and deviates increasingly with decreasing temperature from the GCMC curve, until it reaches a plateau in the low temperature regime. The MF free energy curve instead shows a minimum and increases slightly with decreasing temperature. Only a small discontinuity in the first-order derivative of the average density and grand canonical free energy with respect to temperature can be deduced from the graphs at a temperature of $T^*\approx 0.8$. This value deviates by an order of magnitude from the temperature of the liquid-solid transition at $T^*\approx 0.08$, obtained from the MD and LD calculations. Furthermore, we note that the curves of the average density and grand canonical free energy, computed with the GCMC approach, do not exhibit any characteristics of the liquid-solid transition over the entire temperature range. We explain this with the fact that at lower temperatures the kinetic energy of the particles is reduced and, thus, the probability that a cavity is created or destroyed due to fluctuations becomes smaller. Therefore, it becomes more unlikely that a particle can successfully be added to or eliminated from the system, as we can easily deduce from the creation and destruction probabilities visualized in Fig. 7, and, as a consequence, the GCMC algorithm fails to provide useful results. Our conclusions concord well with the observations made by Orkoulas and Panagiotopoulos [6], who found in case of ionic systems that grand canonical algorithms become increasingly unreliable with decreasing temperature. To overcome these difficulties, special strategies have been conceived to extend the applicability of the GCMC technique to a wider range of parameters, like, e.g., the cavity-biased method of Mezei [44]. New developments essentially based on this approach have recently provided some improved sampling efficiency [45]. However, there is an obvious inherent limitation of the particle-based approaches in their extensibility to the low

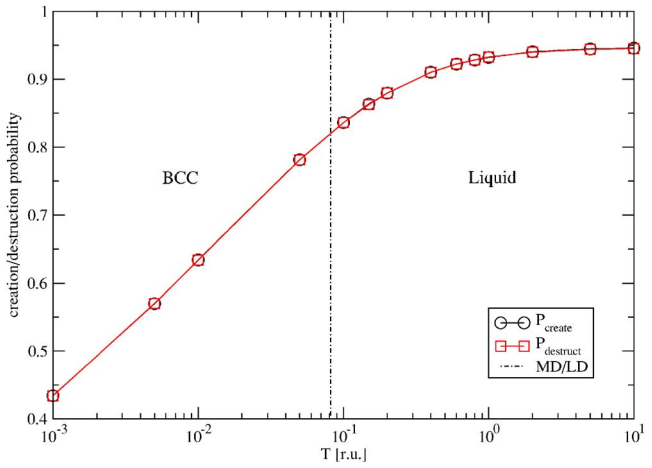

FIG. 7. (Color online) Creation and destruction probabilities, obtained from the GCMC approach, as a function of temperature for the DH intermonomer interaction model.

temperature and/or high density regime, due to their underlying particle exchange algorithm. Other methods make use of extended sampling schemes, in which particles are gradually inserted into the physical system, such as, e.g., the grand canonical molecular dynamics method of Cagin and Pettitt [46] or the method of Attard [47]. However, these methods are unphysical in nature, because they do not sample the true grand canonical distribution function. As a consequence, the convergence to the correct thermodynamic averages can never be guaranteed, and these methods have been found to provide wrong results in several important cases [48]. In conclusion, we see that the GER0 approximation method is a much more reliable method to determine the phase boundaries of the DH model than the MF, GCMC as well as the other grand canonical approaches described previously. Finally, it is also worth pointing out that the computational costs of the GER0 approach are comparable to the ones of the MF approach, but they are much lower than the costs of the standard GCMC approach. The benefit with respect to the GCMC approach becomes the more crucial the higher the degree of sophistication of the polymer model, i.e., the more molecular details are incorporated into the calculation.

V. CONCLUSIONS AND OUTLOOK

In summary, we have demonstrated in this paper on the example of an effective potential model, mimicking the effective interactions between weakly charged polyelectrolyte coils, and a screened Coulomb model, describing the effective intermonomer interactions of Debye-Hückel chains, that the GER0 approach is an efficient low-cost approximation method for functional integrals beyond the MF level of approximation. In particular, we have shown that it provides a far more accurate 0th-order approximation of the grand canonical free energy and related thermodynamic quantities, than the traditional MF approximation over the whole range of chemical potentials, while only requiring a negligible amount of additional computational costs. Moreover, we have demonstrated on the example of the screened Coulomb model that the GER0 approach is also much more reliable compared to the standard MF and grand canonical Monte Carlo approaches, to determine the phase boundaries of potential models with hard-core repulsion. In conclusion, we believe that the GER0 approach can become an appealing alternative to the MF approach in cases, where correlations between the interacting entities are important and where the latter approach fails to provide useful results. Moreover, we believe that our approach opens new perspectives to extend the range of applicability of the grand canonical ensemble to dense liquid and solid phases of complex polymeric materials, like, e.g., biomaterials [11] and foods [49]. Our future work will therefore concentrate on the development and application of the GER methodology to more sophisticated polymer models.

ACKNOWLEDGMENTS

The authors gratefully acknowledge the support of Hans-Jürgen Herrmann offering helpful suggestions and encouragement. The work was also supported by the Russian Foundation for Fundamental Research (N05-03-32251) and Rhodia (France).

APPENDIX A: GER0 APPROXIMATIONS OF THERMODYNAMIC PROPERTIES

The GER0 approximations of simple thermodynamic quantities and fluctuations can be derived in two ways, i.e., via the free energy route (F route) and the radial distribution function route [$g(r)$ route]. In the F route the standard thermodynamic expressions [50] are employed in conjunction with the GER0 approximation of the grand canonical free energy in Eq. (19) or equivalently the grand canonical partition function in Eq. (20). For example, in case of the average particle number we start from the following expression:

$$\langle N\rangle = \frac{z}{\Xi(z,V,\beta)}\left(\frac{\partial \Xi(z,V,\beta)}{\partial z}\right). \tag{A1}$$

Inserting the GER0 approximation of the partition function, given in Eq. (20), into Eq. (A1), we get

$$\langle N\rangle = \frac{V c^{\mathrm{GER}}}{\beta \tilde{\Phi}(\mathbf{p}=0)}, \tag{A2}$$

where in case of the Gaussian model the Fourier transform of the potential is given by

$$\tilde{\Phi}(\mathbf{p}) = \Phi(0)\pi^{3/2}R^3 \exp\left(-\frac{1}{4}R^2|\mathbf{p}|^2\right), \tag{A3}$$

while for the DH potential the Fourier transform is

$$\tilde{\Phi}(\mathbf{p}) = \frac{4\pi\Phi_0}{|\mathbf{p}|^2+\kappa^2}. \tag{A4}$$

The GER0 approximation of the average pressure in the F route can be obtained using the standard thermodynamic formula

$$\langle P\rangle = -\frac{\Omega}{V} = \frac{1}{\beta V}\ln \Xi(z,V,\beta) \tag{A5}$$

and, thus, we get

$$\langle P\rangle = -\frac{\Omega^0_{\mathrm{GER}}}{V}, \tag{A6}$$

where Ω^0_{GER} is given by Eq. (19). Next, we describe how to determine thermodynamic properties within the 0th-order GER approximation using the route via the radial distribution function. To derive the GER0 approximation of the correlation functions, we define the following generating functional by adding a source term to the original field-theoretic representation of the grand canonical partition function given in Eq. (2) [31]:

$$I(z,V,\beta;\psi) = \int d\mu_\Phi[\phi]\exp\left(z\int_V d\mathbf{r}[1+\psi(\mathbf{r})]:e^{i\sqrt{\beta}\phi(\mathbf{r})}:_\Phi\right), \tag{A7}$$

where $\psi(\mathbf{r})$ represents an external source field. With this functional, we can derive the nth-order correlation function using

$$g^{(n)}(\mathbf{r}_1,\ldots,\mathbf{r}_n) = \frac{1}{I(z,V,\beta)}\left.\frac{\delta^n I(z,V,\beta;\psi)}{\delta\psi(\mathbf{r}_1)\cdots\delta\psi(\mathbf{r}_n)}\right|_{\psi=0} = \frac{z^n}{I(z,V,\beta)}\int d\mu_\Phi[\phi]:e^{i\sqrt{\beta}[\phi(\mathbf{r}_1)+\cdots+\phi(\mathbf{r}_n)]}:\exp\left(z\int_V d\mathbf{r}:e^{i\sqrt{\beta}\phi(\mathbf{r})}:_\Phi\right). \tag{A8}$$

The pair correlation function is then given by

$$g^{(2)}(\mathbf{r}_1-\mathbf{r}_2) = \frac{z^2}{I(z,V,\beta)}\int d\mu_\Phi[\phi]:e^{i\sqrt{\beta}[\phi(\mathbf{r}_1)+\phi(\mathbf{r}_2)]}:\exp\left(z\int_V d\mathbf{r}:e^{i\sqrt{\beta}\phi(\mathbf{r})}:_\Phi\right). \tag{A9}$$

Analogously as in case of the derivation of the partition function integral in Sec. II A, the pair correlation function can be rewritten with respect to the new Gaussian measure

$$g^{(2)}(\mathbf{r}_1-\mathbf{r}_2) = \int d\mu_D[\phi]:e^{i\sqrt{\beta}\phi(\mathbf{r}_1)}:_D:e^{i\sqrt{\beta}\phi(\mathbf{r}_2)}:_D e^{W[\phi]}, \tag{A10}$$

with $W[\phi]$ defined as in Eq. (17). We can now easily derive the 0th-order GER approximation of the distribution function by setting $W[\phi]=0$, which provides the radial pair distribution function [32]

$$g(r) = e^{-\beta D(r)}, \tag{A11}$$

where $D(r)$ is defined by Eq. (15) and c^{GER} by Eq. (14). The thermodynamic properties can now easily be obtained by using the standard thermodynamic expressions, formulated in terms of the radial pair distribution function, and inserting the GER0 approximation of the radial pair distribution function given previously. For example, for the average pressure we use

$$\langle P\rangle = \frac{\langle\rho\rangle}{\beta}\left(1-\frac{2}{3}\pi\beta\rho\int_0^\infty g(r)\frac{d\Phi(r)}{dr}r^3dr\right), \tag{A12}$$

with $g(r)$ given by Eq. (A11). It is worth considering in this context that, in contrast to the route via the free energy, determining properties via the radial distribution function permits to take into account second-order terms in the field ϕ with respect to the new Gaussian measure. As a consequence, a higher accuracy in the thermodynamic quantities is expected in the latter case and, therefore, we used for the GER0 calculations the $g(r)$ route throughout the paper, unless explicitly specified otherwise.

APPENDIX B: MEAN-FIELD APPROXIMATIONS OF THERMODYNAMIC PROPERTIES

Analogously as in the GER0 case discussed in the preceding section, the MF approximations of simple thermodynamic quantities and fluctuations can easily be derived using the standard thermodynamic expressions in conjunction with the MF approximation of the grand canonical partition function, given in Eq. (25) or its corresponding free energy. This procedure is called the free-energy route (F route) of the MF approximation. For example, in the case of the average particle number we insert the MF approximation of the partition function, given in Eq. (25), into Eq. (A1) and get

$$\langle N\rangle = zVe^{(\beta/2)\Phi(0)}e^{-c^{\mathrm{MF}}}. \tag{B1}$$

The MF approximation of the average pressure in the F route can be obtained using the standard thermodynamic formula, given in Eq. (A5). As a result, we obtain the following expression for the average pressure:

$$\langle P\rangle = \frac{\langle N\rangle^2\tilde{\Phi}(\mathbf{p}=0)}{2V} + \frac{\langle N\rangle}{V\beta}. \tag{B2}$$

Finally, we note that we obtain similar thermodynamic expressions within the MF approximation using the $g(r)$ route.

[1] M. Hara, *Polyelectrolytes: Science and Technology* (Marcel Dekker, New York, 1993); H. Dautzenberg, W. Jaeger, J. Kotz, B. Philipp, Ch. Seidel, and D. Stscherbina, *Polyelectrolytes: Formation, Characterization, and Application* (Hanser Gardner, Munich, 1994).

[2] M. Konieczky, C. N. Likos, and H. Löwen, J. Chem. Phys. **121**, 4913 (2004).

[3] Q. Wang, T. Taniguchi, and G. H. Fredrickson, J. Phys. Chem. B **108**, 6733 (2004).

[4] M. P. Allen and D. J. Tildesley, *Computer Simulation of Liquids* (Clarendon, Oxford, 1996).

[5] G. H. Fredrickson, *The Equilibrium Theory of Inhomogeneous Polymers* (Clarendon, Oxford, 2006), and references therein.

[6] G. Orkoulas and A. Z. Panagiotopoulos, Fluid Phase Equilib. **83**, 223 (1993), and references therein.

[7] S. A. Baeurle, Comput. Phys. Commun. **157**, 201 (2004).

[8] M. J. Stevens and K. Kremer, Phys. Rev. Lett. **71**, 2228 (1993); J. Chem. Phys. **103**, 1669 (1995).

[9] V. Vlachy and A. D. J. Haymet, J. Chem. Phys. **84**, 5874 (1986); R. Chang and A. Yethiraj, Macromolecules **38**, 607 (2005).

[10] S. A. Baeurle and J. Kroener, J. Math. Chem. **36**, 409 (2004), and references therein.

[11] A. Redondo and R. LeSar, Annu. Rev. Mater. Res. **34**, 279 (2004).

[12] S. Förster, V. Abetz, and A. H. E. Müller, Adv. Polym. Sci. **166**, 173 (2004); A. S. Kimerling, W. E. Rochefort, and S. R. Bhatia, Ind. Eng. Chem. Res. **45**, 6885 (2006).

[13] S. A. Baeurle, T. Usami, and A. A. Gusev, Polymer **47**, 8604 (2006); S. A. Baeurle, A. Hotta, and A. A. Gusev, *ibid.* **47**, 6243 (2006).

[14] F. Schmid, J. Phys.: Condens. Matter **10**, 8105 (1998); G. H. Fredrickson, V. Ganesan, and F. Drolet, Macromolecules **35**, 16 (2002); M. W. Matsen, J. Phys.: Condens. Matter **14**, R21 (2002); J.-M. Caillol, O. Patsahan, and I. Mryglod, Physica A **368**, 326 (2006).

[15] S. F. Edwards, Proc. Phys. Soc. London **85**, 613 (1965).

[16] E. Helfand and Y. Tagami, J. Polym. Sci., Part B: Polym. Lett. **9**, 741 (1971).

[17] I. Borukhov, D. Andelman, and H. Orland, Eur. Phys. J. B **5**, 869 (1998).

[18] R. R. Netz and D. Andelman, Phys. Rep. **380**, 1 (2003).

[19] A.-C. Shi and J. Noolandi, Macromol. Theory Simul. **8**, 214 (1999).

[20] S. Tsonchev, R. D. Coalson, and A. Duncan, Phys. Rev. E **60**, 4257 (1999).

[21] S. A. Baeurle, Phys. Rev. Lett. **89**, 080602 (2002).

[22] S. A. Baeurle, J. Comput. Phys. **184**, 540 (2003).

[23] S. A. Baeurle, Comput. Phys. Commun. **154**, 111 (2003).

[24] R. Baer, M. Head-Gordon, and D. Neuhauser, J. Chem. Phys. **109**, 6219 (1998); S. A. Baeurle, Int. J. Theor. Phys. **41**, 1915 (2002); S. A. Baeurle, J. Math. Chem. **34**, 29 (2003).

[25] G. V. Efimov and G. Ganbold, Phys. Status Solidi B **168**, 165 (1991).

[26] V. Ganesan and G. H. Fredrickson, Europhys. Lett. **55**, 814 (2001); A. Alexander-Katz, A. G. Moreira, and G. H. Fredrickson, J. Chem. Phys. **118**, 9030 (2002).

[27] A. G. Moreira, S. A. Baeurle, and G. H. Fredrickson, Phys. Rev. Lett. **91**, 150201 (2003).

[28] S. A. Baeurle, G. V. Efimov, and E. A. Nogovitsin, Europhys. Lett. **75**, 378 (2006).

[29] G. E. Norman and V. S. Filinov, High Temp. **7**, 216 (1969).

[30] M. Dineykhan, G. V. Efimov, G. Ganbold, and S. N. Nedelko, *Oscillator Representation in Quantum Physics* (Springer, Berlin, 1995).

[31] G. V. Efimov and E. A. Nogovitsin, Physica A **234**, 506 (1996).

[32] S. A. Baeurle, R. Martonak, and M. Parrinello, J. Chem. Phys. **117**, 3027 (2002).

[33] G. V. Efimov and G. Ganbold, Phys. Part. Nucl. **26**, 198 (1995).

[34] A. A. Louis, P. G. Bolhuis, and J. P. Hansen, Phys. Rev. E **62**, 7961 (2000); A. A. Louis, P. G. Bolhuis, J. P. Hansen, and E. J. Meijer, Phys. Rev. Lett. **85**, 2522 (2000).

[35] C. N. Likos, Phys. Rep. **348**, 267 (2001).

[36] F. H. Stillinger and T. A. Weber, J. Chem. Phys. **68**, 3837 (1978).

[37] G. Massiera, L. Ramos, C. Ligoure, and E. Pitard, Phys. Rev. E **68**, 021803 (2003); C. Ligoure, J. Phys.: Condens. Matter **17**, S2911 (2005).

[38] T. B. Liverpool and M. Stapper, Europhys. Lett. **40**, 485 (1997).

[39] B. V. Derjaguin, Kolloid-Z. **69**, 155 (1934); B. V. Derjaguin and L. D. Landau, Acta Physicochim. URSS **14**, 633 (1941); E. J. Verwey and J. T. G. Overbeek, *Theory of the Stability of Lyophobic Colloids* (Elsevier, Amsterdam, 1948).

[40] K. Kremer, M. O. Robbins, and G. S. Grest, Phys. Rev. Lett. **57**, 2694 (1986), and references therein; V. Vlachy, C. Pohar, and A. D. J. Haymet, J. Chem. Phys. **88**, 2066 (1988); J. S. Rowlinson, Physica A **156**, 15 (1989), and references therein; N. Pistor and K. Kremer, *ibid.* **201**, 171 (1993).

[41] M. O. Robbins, K. Kremer, and G. S. Grest, J. Chem. Phys. **88**, 3286 (1988), and references therein.

[42] S. A. Baeurle, G. V. Efimov, and E. A. Nogovitsin, J. Chem. Phys. **124**, 224110 (2006).

[43] M. Dijkstra and R. van Roij, J. Phys.: Condens. Matter **10**, 1219 (1998).

[44] M. Mezei, Mol. Phys. **40**, 901 (1980).

[45] R. M. Shroll and D. E. Smith, J. Chem. Phys. **110**, 8295 (1999), and references therein.

[46] T. Cagin and B. M. Pettitt, Mol. Simul. **6**, 5 (1991); Mol. Phys. **72**, 169 (1991); J. Ji, T. Cagin, and B. M. Pettitt, J. Chem. Phys. **96**, 1333 (1992).

[47] P. Attard, J. Chem. Phys. **107**, 3230 (1997).

[48] S. Weerasinghe and B. M. Pettitt, Mol. Phys. **82**, 897 (1994).

[49] R. Mezzenga, P. Schurtenberger, A. Burbidge, and M. Michel, Nat. Mater. **4**, 729 (2005).

[50] K. Huang, *Statistical Mechanics* (Wiley, New York, 1987).